

# Fast and accurate computation of partially coherent imaging by stacked pupil shift operator

Yaogang Lian, Xin Zhou

Luminescent Technologies, 2471 East Bayshore Road Suite 600, Palo Alto, CA 94303

## ABSTRACT

In this paper, the stacked pupil shift operator approach to partially coherent imaging as first introduced by Yamazoe<sup>1</sup> has been further pursued and investigated with a focus on its practical performances in lithographic simulations. The stacked pupil shift operator  $\mathcal{P}$  is a singular matrix obtained by stacking pupil functions that are shifted according to the illumination condition. The transmission cross coefficient (TCC) matrix can then be constructed in an elegant fashion as  $\text{TCC} = \mathcal{P}^\dagger \mathcal{P}$ . The new development presented in this paper utilizes a matrix multiplication technique to speed up the computation of TCC matrix by tenfolds on average. This enables fast and accurate generation of TCC kernels for complicated illumination source shapes where a large number of source points are required to obtain good accuracy.

**Keywords:** TCC, stacked pupil shift operator, fast lithography simulation

## 1. INTRODUCTION

Partially coherent imaging as first formulated by Hopkins<sup>2</sup> using the four-dimensional Transmission-Cross-Coefficient (TCC) matrix has been the foundation of lithography simulations for decades. With the assumption that mask diffraction orders are invariant with respect to the angle of incidence of illuminating light, the Hopkins approach computes the light intensity distribution on the image plane by interfering pairs of light waves traveling with different angles, weighed by the TCC. Since all the illumination and pupil information have been absorbed into the four-dimensional TCC matrix, the Hopkins's approach has the advantage of computing image intensities for different mask patterns without recomputing the TCC matrix as long as the optical setup remains the same. This is especially valuable for Inverse Lithography (ILT) where mask inversion is often carried out in many iterations with the optical settings fixed.

However, straightforward numerical calculations of the Hopkins's equation demands large computer memory due to the storage of the four-dimensional TCC matrix and long computation time due to the quadruple integral in the Hopkins's equation. These memory and computation time constraints can be significantly reduced by the Sum Of Coherent System (SOCS) decomposition method<sup>3</sup> which decomposes the four-dimensional TCC matrix into eigenvalues and eigenfunctions of the aerial image and stores only a small subset of eigenvalues and eigenfunctions to produce an approximate aerial image with high accuracy. Although the SOCS decomposition method has significantly reduced the memory and computation time requirements during the step of computing aerial image from the TCC matrix, the SOCS method still needs to compute the four-dimensional TCC matrix and its eigenvalue decomposition as a prerequisite step. With the introduction of increasingly complicated illumination sources the computation of the TCC matrix using the traditional way of integration over the overlapped area of the effective source, the pupil function and the pupil function conjugate, has shown its limits.

An alternative approach to partially coherent imaging is the source points integration method, or Abbe's method. In Abbe's method the aerial image is computed by an incoherent summation of all light intensity emitted by a set of mutually incoherent point sources. Abbe's method uses Fast Fourier transform (FFT) algorithm to compute each component image arising from an effective point source and does not require the TCC matrix, thus the speed of Abbe's method solely depends on the number of illumination source points. However, Abbe's method is intrinsically incompatible with inverse lithography since the component image computation depends on the mask pattern thus has to be redone each time the mask pattern is changed, resulting in a very lengthy inversion time.

In a recent paper<sup>1</sup> Yamazoe introduced a new approach to partially coherent imaging which possesses the advantage of both Abbe's method and SOCS. At the core of this new method is the so-called stacked pupil shift

operator  $\mathcal{P}$ , a singular matrix obtained by stacking pupil functions that are shifted according to the illumination condition. By writing the analytical form of Abbe’s method into an equivalent matrix form, it was shown that the TCC matrix can simply be constructed by the product of the stacked pupil shift operator  $\mathcal{P}$  and its Hermitian conjugate  $\mathcal{P}^\dagger$ . This discovery not only provides important insights into the relationship between Abbe’s method and the Hopkins’s approach, but also sparks a faster and more natural way of computing the TCC matrix numerically. When the number of source points is small, Yamazoe showed that significant speed improvement can be achieved by applying the singular value decomposition (SVD) to the stacked pupil shift operator  $\mathcal{P}$  instead of the TCC matrix, thus completely eliminating the need to compute or store the four-dimensional TCC matrix. Aerial image is then computed in the same way as in SOCS using the eigenvalues and eigenfunctions derived from the SVD of the stacked pupil shift operator.

However, real life lithographic simulations rarely use a *small* number of source points. Even for the traditional illumination source shapes such as annular, quasar, or dipole sources, the number of source sampling points required to obtain good simulation accuracy is often over a thousand. As increasingly complicated illumination source shapes are designed and used in production to further push down the lithographic limits, the number of source points needed to accurately sample the user source in order to maintain reasonable simulation accuracy also gets larger. When the number of source points is comparable to the two-dimensional grid size in the frequency domain ( $N^2$ ) the time savings from applying the SVD to the stacked pupil shift operator diminish. In the cases where the number of source points exceed the two-dimensional grid size in the frequency domain ( $N^2$ ) the stacked pupil shift operator approach may even be slower than the traditional Hopkins’s approach.

In this paper the stacked pupil shift operator approach to partially coherent imaging has been further pursued and investigated with a focus on its practical performances in lithographic simulations. Section 2 starts with a review of the stacked pupil shift operator approach and explains the deep relationships between this new approach and the traditional Hopkins’s approach and Abbe’s method. Practical implementation methods are then presented showing that the speed advantage of this new approach can be maintained even with a large number of source points, through the use of fast matrix multiplication techniques.

Section 3 compares simulation results using three different approaches to partially coherent imaging, namely the stacked pupil shift operator approach, the Hopkins’s approach, and Abbe’s method. It will be shown that the stacked pupil shift operator approach is considerably faster than the traditional Hopkins’s approach where the TCC matrix is computed by evaluating the double integral, even in the cases where complicated user-defined illumination source shapes are used which require a large number of source sampling points. Interestingly the speed improvement of the stacked pupil shift operator approach doesn’t come with a tradeoff in simulation accuracy, on the contrary, it will be shown that the new approach is at the same time more accurate than the traditional Hopkins’s approach when compared to the simulation result of Abbe’s method. The simultaneous improvement on both speed and accuracy doesn’t come as a surprise but reflects the power of the insights that the stacked pupil shift operator is a fundamental operator in partially coherent imaging.

## 2. THEORY AND IMPLEMENTATION METHODS

In this section the theory of the stacked pupil shift operator approach to partially coherent imaging is reviewed and implemented with special emphasis on modeling optical effects such as aberration, apodization, and light intensity distribution and polarization state of the effective light source. Following the common convention, the coordinate system in this section is denoted by  $(x, y)$  in the spatial domain while denoted by  $(f, g)$  in the frequency domain.

### 2.1 Overview of Stacked Pupil Shift Operator

In a simplified lithographic imaging scheme the aerial image is formed in the following steps:

1. The light emitted from the illumination source goes through the condenser lens and is transformed into mutually incoherent plane waves;
2. These plane waves are diffracted by the lithographic mask into different directions, so-called diffraction orders, or mask spectrum;

3. The diffracted light is cut off by the projection pupil and redirected towards the wafer where the aerial image is formed;
4. The aerial image is obtained by an incoherent superposition of light intensity distributions from all plane waves.

The Hopkins's approach is based on the assumption that mask diffraction orders are independent of the direction of the incident light, thus the mask spectrum due to an off-axis source point  $s$  is simply described by  $M(f - f_s, g - g_s)$ , a shifted version of the mask spectrum  $M(f, g)$  due to an on-axis source point. The light intensity distribution  $I_s(x, y)$  due to the source point  $s$  can therefore be described by

$$I_s(x, y) = \left| \iint_{-\infty}^{+\infty} P(f, g) M(f - f_s, g - g_s) e^{-i2\pi(fx + gy)} df dg \right|^2, \quad (1)$$

where  $P(f, g)$  is the pupil function.

The total aerial image is obtained by an incoherent superposition of light intensities from all source points and thus described by the Hopkins's equation:<sup>2</sup>

$$I(x, y) = \iint \text{TCC}(f', g', f'', g'') M(f', g') M^*(f'', g'') e^{-i2\pi[(f' - f'')x + (g' - g'')y]} df' dg' df'' dg'', \quad (2)$$

where the TCC is represented as

$$\text{TCC}(f', g', f'', g'') = \iint J(f_s, g_s) P(f_s + f', g_s + g') P^*(f_s + f'', g_s + g'') df_s dg_s \quad (3)$$

with  $J(f_s, g_s)$  denoting the source point intensity distribution.

The traditional way to evaluate the TCC in Equation (3) requires an integration over the overlapped area of three circles - the effective illumination source  $J(f_s, g_s)$ , the pupil function  $P(f_s + f', g_s + g')$  and the conjugate of pupil function  $P^*(f_s + f'', g_s + g'')$ , for each element of the four-dimensional TCC matrix. For standard illumination source shapes such as circular, annular, quasar, and dipole sources, the analytical form of the source shape can be utilized to facilitate the integration; however, as more complicated or freeform illumination source shapes are introduced, the traditional integration approach is getting increasingly cumbersome and slow.

The important discovery made by Yamazoe<sup>1</sup> is that Equation (3) can be evaluated without integration. By exploring the matrix representation of Equation (3), a fundamental operator  $\mathcal{P}$  in partially coherent imaging was introduced and the TCC matrix can be constructed by a simple matrix multiplication using the operator  $\mathcal{P}$  and its Hermitian conjugate. This new formulation of partially coherent imaging can be derived by rewriting Eqs. (1), (2) and (3) into their equivalent matrix representations. Suppose the number of sampling points in the pupil plane is  $(M, N)$ , Equation (1) can be rewritten in a discretized form as

$$I_s(x, y) = \left| \sum_{i=1}^M \sum_{j=1}^N P(f_i, g_j) M(f_i - f_s, g_j - g_s) e^{-i2\pi(f_i x + g_j y)} \right|^2. \quad (4)$$

Define  $f'_i = f_i - f_s, g'_j = g_j - g_s$ , the above equation can be transformed as

$$\begin{aligned} I_s(x, y) &= \left| \sum_{i=1}^M \sum_{j=1}^N P(f'_i + f_s, g'_j + g_s) M(f'_i, g'_j) e^{-i2\pi[(f'_i + f_s)x + (g'_j + g_s)y]} \right|^2 \\ &= \left| \sum_{i=1}^M \sum_{j=1}^N P(f'_i + f_s, g'_j + g_s) M(f'_i, g'_j) e^{-i2\pi(f'_i x + g'_j y)} \right|^2. \end{aligned} \quad (5)$$

Now we see that the pupil function is shifted due to illumination source conditions.

The double summation in Equation (5) can be written in the matrix notation if we define a stacking operator  $\mathbf{Y}$  that reshapes a two-dimensional matrix into a one-dimensional vector. A simple implementation of the stacking operator is to place each row of the matrix sequentially into a one-dimensional array. Thus we can define the stacked diffracted plane wave vector  $\hat{M}$  as

$$\hat{M} = \mathbf{Y} \left[ M(f'_i, g'_j) e^{-i2\pi(f'_i x + g'_j y)} \right] = \begin{pmatrix} M(f'_1, g'_1) e^{-i2\pi(f'_1 x + g'_1 y)} \\ \vdots \\ M(f'_1, g'_N) e^{-i2\pi(f'_1 x + g'_N y)} \\ M(f'_2, g'_1) e^{-i2\pi(f'_2 x + g'_1 y)} \\ \vdots \\ M(f'_2, g'_N) e^{-i2\pi(f'_2 x + g'_N y)} \\ \vdots \\ M(f'_M, g'_N) e^{-i2\pi(f'_M x + g'_N y)} \end{pmatrix}. \quad (6)$$

Similarly we can define the stacked pupil shift vector  $\mathcal{P}_s$  as

$$\begin{aligned} \mathcal{P}_s &= \mathbf{Y} [P(f'_i + f_s, g'_j + g_s)] \\ &= \left( P(f'_1 + f_s, g'_1 + g_s), \dots, P(f'_1 + f_s, g'_N + g_s), P(f'_2 + f_s, g'_1 + g_s), \dots, \right. \\ &\quad \left. P(f'_2 + f_s, g'_N + g_s), \dots, P(f'_M + f_s, g'_N + g_s) \right). \end{aligned} \quad (7)$$

Now we can rewrite Equation (5) in a very compact form as

$$I_s(x, y) = \left| \mathcal{P}_s \hat{M} \right|^2 = \hat{M}^\dagger (\mathcal{P}_s^\dagger \mathcal{P}_s) \hat{M}. \quad (8)$$

The total aerial image can thus be obtained by the incoherent superposition of light intensity distributions from all source points  $s = 1, \dots, N_s$ , weighed by the source point intensity  $J_s$ :

$$\begin{aligned} I(x, y) &= \sum_{s=1}^{N_s} J_s \cdot I_s(x, y) \\ &= \hat{M}^\dagger \left( \sum_{s=1}^{N_s} J_s \mathcal{P}_s^\dagger \mathcal{P}_s \right) \hat{M} \\ &= \hat{M}^\dagger (\mathcal{P}^\dagger \mathcal{P}) \hat{M}, \end{aligned} \quad (9)$$

where

$$\mathcal{P} = \begin{pmatrix} \sqrt{J_1} \mathcal{P}_1 \\ \sqrt{J_2} \mathcal{P}_2 \\ \vdots \\ \sqrt{J_{N_s}} \mathcal{P}_{N_s} \end{pmatrix} \quad (10)$$

is the so-called stacked pupil shift operator. It's clear that the operator  $\mathcal{P}$  can be easily constructed by the stacked pupil functions shifted due to illumination source points.

Now we return to Equation (2) and rewrite it in a discretized form,

$$I(x, y) = \sum_{i_1=1}^M \sum_{j_1=1}^N \sum_{i_2=1}^M \sum_{j_2=1}^N \text{TCC}(f'_{i_1}, g'_{j_1}, f''_{i_2}, g''_{j_2}) M(f'_{i_1}, g'_{j_1}) M^*(f''_{i_2}, g''_{j_2}) e^{-i2\pi[(f'_{i_1} - f''_{i_2})x + (g'_{j_1} - g''_{j_2})y]}. \quad (11)$$

Using the stacked diffracted plane wave vector  $\hat{M}$  as defined earlier, this equation can be rewritten in a more compact matrix form as

$$I(x, y) = \hat{M}^\dagger \text{TCC} \hat{M}. \quad (12)$$

Compared to Equation (9), the relationship between the TCC matrix and the stacked pupil shift operator  $\mathcal{P}$  is now clear:

$$\text{TCC} = \mathcal{P}^\dagger \mathcal{P}, \quad (13)$$

i.e. the TCC matrix is simply a product of the stacked pupil shift operator  $\mathcal{P}$  and its Hermitian conjugate. Since the operator  $\mathcal{P}$  can be rapidly constructed by shifting the pupil function with respect to illumination source points, this relationship leads to the fast TCC matrix computation.

## 2.2 Implementation Methods

The stacked pupil shift operator approach to partially coherent imaging can be easily implemented to handle real optical conditions such as the aberration, apodization, and light intensity distribution and polarization state of the effective light source. The source intensity distribution  $J(f, g)$  is already taken into account in the derivation of Equation (9) in the last subsection. The aberration and apodization effects can also be easily modeled in the pupil function:

$$P(f, g) = \text{circ}(f, g) o(f, g) e^{-i2\pi W(f, g)}, \quad (14)$$

where  $o(f, g)$  is the apodization function and  $W(f, g)$  is the aberration function.

The extension of the stacked pupil shift operator  $\mathcal{P}$  to include the polarization state of the illumination source is also straightforward. Three kinds of pupil functions  $P^x, P^y$ , and  $P^z$  can be defined to capture the vector imaging effects and correspondingly we have three kinds of stacked pupil shift operator  $\mathcal{P}^x, \mathcal{P}^y$ , and  $\mathcal{P}^z$ . The full stacked pupil shift operator  $\mathcal{P}$  can be simply constructed by

$$\mathcal{P} = \begin{pmatrix} \mathcal{P}_x \\ \mathcal{P}_y \\ \mathcal{P}_z \end{pmatrix}. \quad (15)$$

To obtain the final aerial image with the SOCS scheme, eigenvalues and eigenfunctions of the TCC matrix need to be computed. Yamazoe proposed<sup>1</sup> to apply the SVD directly to the stacked pupil shift operator  $\mathcal{P}$  and thus completely eliminate the need to compute or store the TCC matrix. When a small number of source points is used, this method can save considerable computation time because the stacked pupil shift matrix  $\mathcal{P}$  has a much smaller size compared to the TCC matrix. However, in practical lithographic simulations the number of source points required to achieve reasonably good simulation accuracy is often quite large, due to the more and more prevalent uses of user-measured source maps or complicated illumination source shapes. When the number of source points is comparable to or even larger than the sampling grid size in the pupil plane, applying the SVD to the operator  $\mathcal{P}$  will no longer be more efficient than simply decomposing the TCC matrix itself.

So the practical implementation of the stacked pupil shift operator approach can not really rely on the speed boost due to bypassing the TCC matrix; instead, the TCC matrix still needs to be computed and decomposed. However, the elegant formulation of the TCC matrix in Equation (13) still makes possible a significant speed improvement over the traditional Hopkins's approach where a double integral has to be evaluated for each element in the TCC matrix. It's observed from Equation (13) that the TCC matrix is computed by a single matrix multiplication step which consumes most of the computation time. Therefore highly optimized matrix multiplication routines can be utilized to achieve the desired speed advantage. A carefully constructed matrix multiplication routine can be tens of times faster than one constructed in the most straightforward way. These routines can be obtained from publicly available linear algebra packages such as Automatically Tuned Linear Algebra Software (ATLAS).

## 3. SIMULATION RESULTS

In this section numerical simulation results from the stacked pupil shift operator implementation as described in Section 2.2 are compared to those from the traditional Hopkins's approach and Abbe's method. Special emphasis is given to the practicality of these simulation experiments.

### 3.1 Accuracy Tests on a Two-dimensional Contact Array

The first set of simulation experiments is designed to test the simulation accuracy of our stacked pupil shift operator implementation on simple mask patterns such as a two-dimensional contact array. The mask used in this simulation is an attenuated Phase Shifting Mask (PSM) with transmission of 6% using standard MoSi absorber. As shown in Fig. 1(a), each contact on the mask has a dimension of 150 nm on both sides and the contact array is periodic in both dimensions. The mask is in dark field so the contacts are actually clear apertures in a dark background. The numerical aperture of the projection optics is 0.93 and the exposure wavelength is 193 nm. Immersion fluid with a refractive index of 1.436 is used on the image side.

Fig. 1(b), (c) and (d) show the three kinds of illumination source shapes used in this simulation experiment - a quasar source with two fans, a quadrupole source and a user-measured quasar source with four fans. Y-polarization is used for all three illumination sources. To obtain good simulation accuracy, 800 source points are used to sample the parametric quasar source, 2048 source points for the quadrupole source, and 2021 source points for the user-measured quasar source. The sampling grid in the pupil plane is of size  $39 \times 39$  thus the number of source points is comparable to (in the case of the parametric quasar source) or even more than (in the cases of the quadrupole source and user-measured quasar source) the size of the sampling grid in the pupil plane.

To compare the aerial images from three approaches namely the stacked pupil shift operator approach, the Hopkins's approach and Abbe's method, a cutline is drawn across the center of a contact and the intensities along the cutline are plotted in Fig. 2. The three rows of plots in Fig. 2 correspond to the three illumination source shapes as discussed earlier. In each row the left-hand plot is the intensity comparison along the whole cutline through a contact while the right-hand plot is a close-up view of the peak in the left-hand plot for a better visual comparison. All plots in Fig. 2 show that the stacked pupil shift operator approach has better simulation accuracy than the traditional Hopkins's approach when compared to the simulation results from the Abbe's method. Note that both the stacked pupil shift operator approach and the Hopkins's approach use 128 TCC kernels to construct the aerial image.

Quantitatively, we can define the relative difference between the simulated intensities as

$$R = \frac{\text{Largest difference between two intensity curves along the cutline}}{\text{Largest intensity along the cutline}}. \quad (16)$$

Thus for the parametric quasar source in the first row of Fig. 2, the relative intensity difference between the Hopkins's approach and the Abbe's method is 0.56% while this number drops to 0.07% when the stacked pupil shift operator approach is used. Similarly for the quadruple source in the second row in Fig. 2, the relative intensity difference compared to Abbe's method is 0.35% when the Hopkins's approach is used, and is 0.18% when the stacked pupil shift operator approach is used. Finally, for the user-measured quasar source in the third row in Fig. 2, the relative difference is 0.98% for the Hopkins's approach and 0.59% for the stacked pupil shift operator approach. These results clearly show that the stacked pupil shift operator approach have better simulation accuracy than the Hopkins's approach when compared to the simulation results from the Abbe's method.

### 3.2 Accuracy Tests on a Complicated Mask Pattern

Next, simulation results on a more complicated mask pattern are presented. As shown in Fig. 3(a) the complicated mask pattern includes features that interact with each other such as line ends, inner and outer corners. The mask stack used here is the typical CoG. The numerical aperture of the projection optics is 1.35 and the exposure wavelength is 193 nm. Immersion fluid with a refractive index of 1.436 is used on the image side. Fig. 3(b) illustrates the illumination source used in this simulation which is a user-measured cross-pole source. The colors on the source map represent the source intensity distribution. In order to obtain good simulation accuracy, 2000 source points are sampled from the source map.

Fig. 4(a) shows the aerial image computed by the Abbe's method with the largest intensity normalized to 1.0. Fig. 4(b) shows the difference of aerial images between the stacked pupil shift operator approach and the Abbe's method. It can be seen that for most regions, the difference of aerial images is less than 0.5%. The maximum difference of 1% occurs in the dense region where local interactions make the aerial image approximation less accurate.

### 3.3 Speed Tests

Finally, a set of simulation experiments are carried out to test the speed performance of the stacked pupil shift operator approach for practical lithographic simulations. The runtime from this new approach is compared to that of the Hopkins’s approach. The mask pattern used in these simulations is the same pattern as used in Section 3.2 which entails real-life lithographic features such as line-ends, inner and outer corners. The numerical aperture of projection optics and exposure wavelength are also the same as in Section 3.2. Three simulations are carried out for this study which include a scalar imaging simulation, a vector imaging simulation using a parametric quasar source which requires a modest number of source points, a vector imaging simulation using a user-measured illumination source as illustrated in Fig. 3(b) with a total of 2000 source points. The last simulation most reflects real-life lithographic simulation conditions thus the metrics for the last simulation is the most important. All three simulations are carried out on the same desktop computer with a fully devoted CPU running at 2.8 GHz for a fair comparison. The runtime measurements for all three simulations are summarized in Table 1.

Table 1. Normalized runtime of three simulations

	Hopkins	Stacked pupil	Speedup ratio
Scalar imaging with parametric source	1.00	0.53	1.9X
Vector imaging with parametric source	4.01	0.86	4.7X
Vector imaging with user-measured source	23.44	1.28	18X

Therefore for all three simulations the stacked pupil shift operator approach is considerably faster than the Hopkins’s approach. The speedup for the case of vector imaging with user-measured illumination source, which most resembles real-life lithographic simulation conditions, is as much as 18X. This result has shown the significance of the stacked pupil shift operator approach in the future of fast lithographic simulations.

## 4. CONCLUSION

In this paper the stacked pupil shift operator approach to partially coherent imaging has been further developed and implemented with a focus on its practical performances in lithographic simulations. Practical implementation methods are discussed and it has been shown that the speed advantage of this new approach can be maintained even when the number of illumination source points is large. Simulation results have shown simultaneous improvement on both speed and accuracy using this new approach, showing that the stacked pupil operator approach is a fundamentally more efficient numerical computation method for partially coherent imaging.

## REFERENCES

- [1] Yamazoe, K., “Computation theory of partially coherent imaging by stacked pupil shift matrix,” *J. Opt. Soc. Am. A* **25**, 3111–3119 (2008).
- [2] Hopkins, H. H., “On the diffraction theory of optical image,” *Proc. R. Soc. London, Ser. A* **217**, 408–432 (1953).
- [3] Cobb, N. B., “Fast optical and process proximity correction algorithms for integrated circuit manufacturing,” *Ph.D. dissertation* (Electrical Engineering and Computer Science, University of California, Berkeley, 1998).

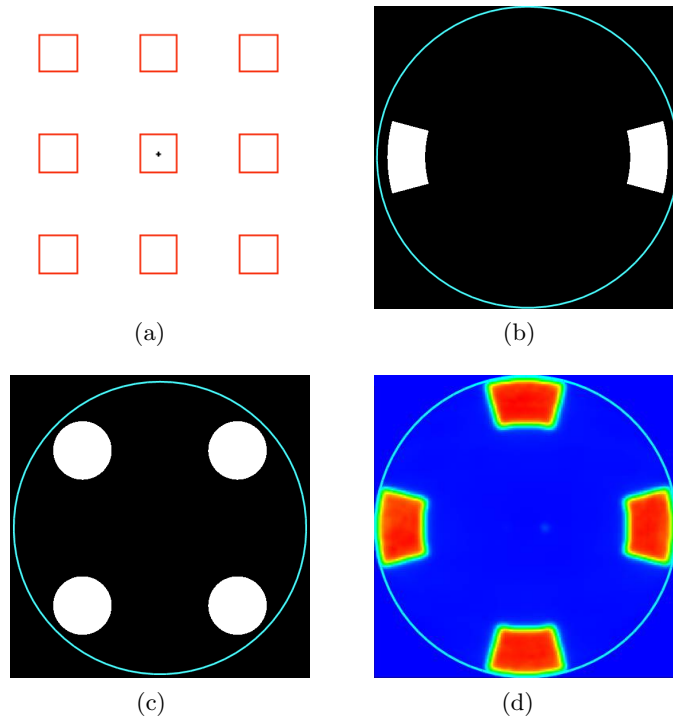
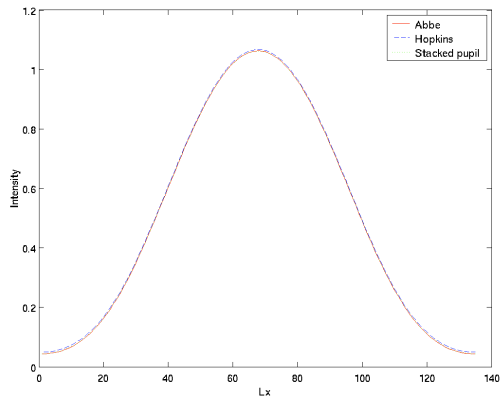
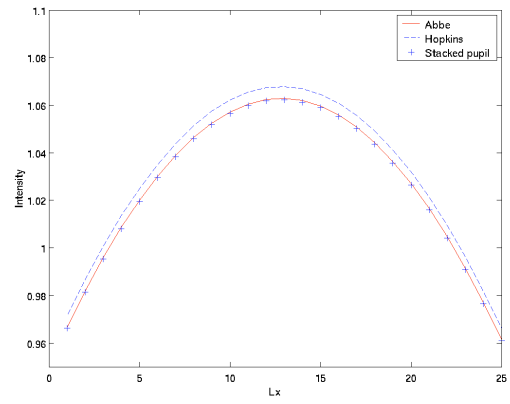


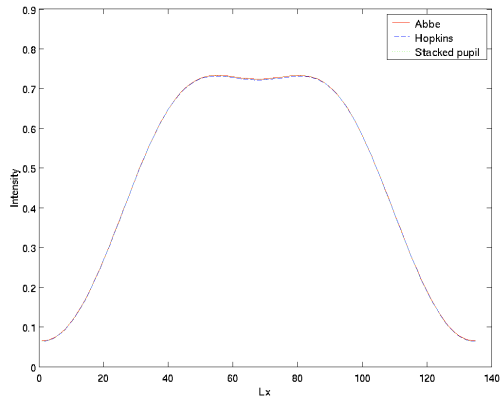
Figure 1. Mask pattern and illumination source shapes. (a) The mask pattern is a two-dimensional contact array with each contact the size of a 150 nm square. Periodic boundary condition is applied to both directions on the mask. (b) Illustration of the parametric quasar source with two fans. (c) Illustration of the quadrupole source. (d) Illustration of the user-measured quasar source with four fans. The colors represent source intensity distribution.



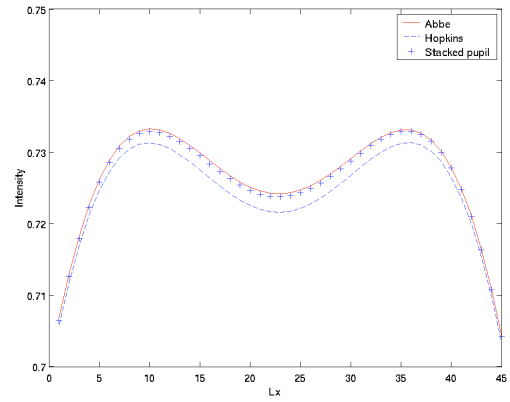
(a)



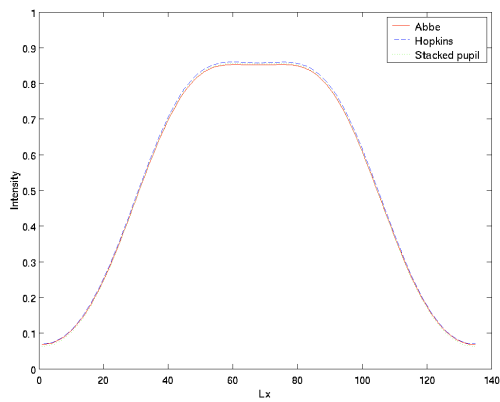
(b)



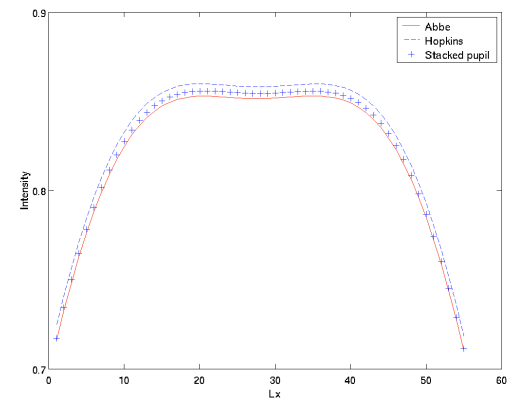
(c)



(d)



(e)



(f)

Figure 2. Comparison of intensities along a cutline drawn across the center of a contact. The intensities are computed by three different approaches namely the stacked pupil shift operator approach, the Hopkins's approach, and the Abbe's method. (a) Intensity comparison for the case of the parametric quasar source. (b) A close-up view of the peak in (a). (c) Intensity comparison for the case of the quadrupole source. (d) A close-up view of the peak in (c). (e) Intensity comparison for the case of the user-measured quasar source. (f) A close-up view of the peak in (e).

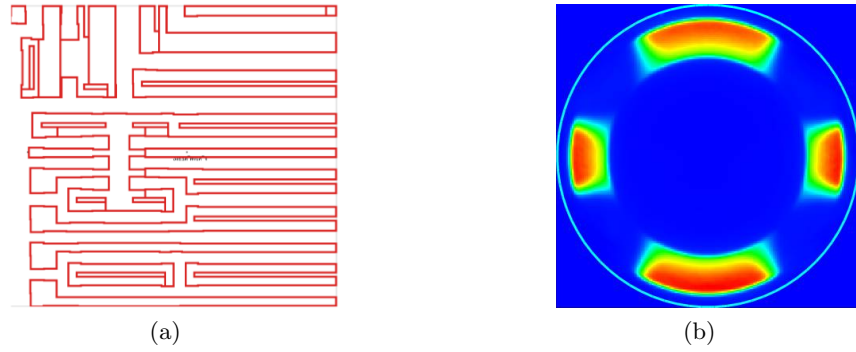


Figure 3. Mask pattern and illumination source. (a) The mask pattern is a two-dimensional complicated pattern with line ends and corners. (b) Illustration of the user-measured illumination source map which is a cross-pole in this case. The colors represent source intensity distribution.

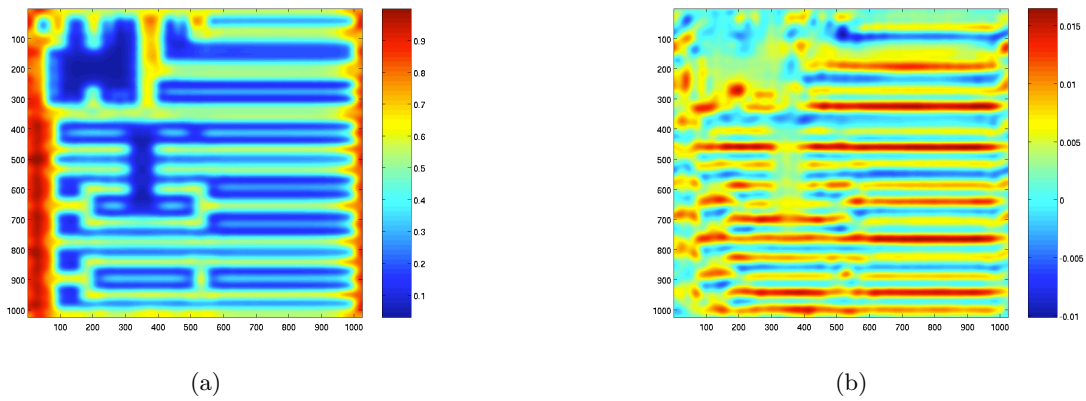


Figure 4. Comparison of aerial images. (a) Aerial image from Abbe's method with the largest intensity normalized to 1.0. (b) Difference of aerial images between the stacked pupil shift operator approach and the Abbe's method.